Search for Scalar Leptoquarks in the Acoplanar Jet Topology with the DØ Detector

The DØ Collaboration
URL: http://www-d0.fnal.gov

(Dated: March 27, 2006)

A search for leptoquarks has been performed in 310 pb^{-1} of data from $p\bar{p}$ collisions at a center-of-mass energy of 1.96 TeV, collected by the DØ detector at the Fermilab Tevatron. The topology analyzed consists of acoplanar jets with missing E_T. The data show good agreement with the standard model expectations, and a mass lower limit of 136 GeV has been set at 95% CL for a scalar leptoquark decaying exclusively into a quark and a neutrino

Preliminary Results for Winter 2006 Conferences

I. INTRODUCTION

Topologies involving jets and missing transverse energy have been widely investigated in the past to search for signals of new phenomena in $p\bar{p}$ collisions. In this note, a search for scalar leptoquarks in the acoplanar jet topology is reported, using $310\,\mathrm{pb}^{-1}$ of data collected at a center-of-mass energy of 1.96 TeV with the upgraded DØ detector [1] during Run II of the Fermilab Tevatron.

Many extensions of the Standard Model (SM) which aim at explaining the apparent symmetry between quarks and leptons predict the existence of leptoquarks (LQ). These new particles are bosons which carry the quantum numbers of a quark-lepton system. They are expected to decay into a quark and a charged lepton with a branching fraction β, or into a quark and a neutrino with a branching fraction $(1-\beta)$. The search reported in this note concentrates on scalar leptoquarks which decay 100% of the time into a quark and a neutrino ($\beta = 0$).

At hadron colliders, leptoquarks can be pair produced, dominantly by $q\bar{q}$ annihilation and gluon-gluon fusion. The resulting final state, for $\beta = 0$, consists of a pair of quark jets, with missing energy carried away by the two neutrinos. With $85\,\mathrm{pb}^{-1}$, a preliminary mass lower limit of 109 GeV had been set by DØ [2], and the CDF collaboration has published a lower limit of 117 GeV, based on $191\,\mathrm{pb}^{-1}$ [3]. Here and in the following, all limits quoted are at the 95% confidence level.

II. DATA SAMPLE

For the search reported in this note, data collected from April 2003 to August 2004 have been analyzed. The Jets + $\not\!\!E_T$ trigger used was not available previously in Run II. At the first level, it selects events in which at least three trigger towers record a transverse energy in excess of 5 GeV. At the second and third levels, requirements are placed on $\not\!\!H_T$, the transverse energy missing to the reconstructed jets ($\not\!\!H_T = |\sum_{jets} \vec{p}_T|$). The $\not\!\!H_T$ thresholds are 20 and 30 GeV at Levels 2 and 3, respectively. About 20% of the data sample was recorded with the additional requirement at Levels 2 and 3 that the acoplanarity between the two leading jets be smaller than 170°, where the acoplanarity is defined as the difference between the two jet azimuthal angles. For the subsequent data selection, it was required that no major component of the detector show any sign of degraded performance. This leaves a total available integrated luminosity of $310\,\mathrm{pb}^{-1}$.

The offline analysis utilizes jets reconstructed with the Run II cone algorithm, with a radius of 0.5 in η-ϕ space, appropriately corrected for the jet energy scale. The so-called good jets are further selected by general quality criteria essentially based on the jet longitudinal profile. In the following, the qualifier "good" in front of "jet" is dropped; it will be restored only in case of ambiguities. Only good jets enter the calculation of kinematic quantities such as $\not\!\!H_T$. The missing transverse energy $\not\!\!E_T$ is calculated from all calorimeter cells, corrected for the energy scale of reconstructed jets and electrons, and for the presence of reconstructed muons.

The sample of ~ 14 million events collected with the Jets + $\not\!\!E_T$ trigger was reduced to a more manageable size by requiring the following criteria to be satisfied:

- $\not\!\!H_T > 40\,\mathrm{GeV}$;
- $\not\!\!E_T > 40\,\mathrm{GeV}$;
- at least two jets;
- $\Delta\Phi < 165°$;
- $|z_{PV}| < 60\,\mathrm{cm}$,

where $\Delta\Phi$ is the acoplanarity of the two leading jets and z_{PV} is the longitudinal position of the primary vertex with respect to the detector center.

Events in which the presence of obvious calorimeter noise could be detected were rejected, as well as those containing at least one jet not rated as good and with a transverse energy larger than 15 GeV. The inefficiency associated with these quality criteria was measured on events selected at random beam crossings (zero-bias events), and also on events collected with an unbiased trigger and containing exactly two jets back-to-back when projected on the plane transverse to the beam.

At this point, 306,937 events survive.

TABLE I: Standard model processes, numbers of events generated, cross sections, and numbers of events expected after all cuts. For the Z+jet(s) processes, the number of events generated and the cross section correspond to the [60-130] GeV $Z/\gamma^\star$ mass range, while all masses from 10 to 250 GeV are taken into account for the number of events expected after all cuts. The errors are statistical only.

SM process	events generated	cross section (pb)	events expected
$Z \to \nu\nu +$ jet jet	104 500	173	34.6 ± 4.3
$W \to \tau\nu +$ jet	97 750	840	$0^{+2.7}_{-0}$
$W \to \tau\nu +$ jet jet	30 250	292	11.0 ± 5.8
$W \to \mu\nu +$ jet jet	51 750	292	12.9 ± 4.8
$W \to e\nu +$ jet	145 500	840	1.7 ± 1.7
$W \to e\nu +$ jet jet	53 500	292	9.4 ± 4.0
$Z \to \tau\tau +$ jet	96 500	81.1	$0^{+0.3}_{-0}$
$Z \to \tau\tau +$ jet jet	102 000	28.3	0.1 ± 0.1
$Z \to \mu\mu +$ jet jet	269 500	28.3	0.1 ± 0.1
$Z \to ee +$ jet	186 750	81.1	$0^{+0.1}_{-0}$
$Z \to ee +$ jet jet	203 450	28.3	0.1 ± 0.1
$t\bar{t} \to bbqq\ell\nu$	191 300	2.9	1.3 ± 0.1
$t\bar{t} \to bb\ell\nu\ell\nu$	57 500	0.7	0.6 ± 0.1
WW	50 000	11.5	0.6 ± 0.2
WZ	53 000	3.5	0.3 ± 0.1
ZZ	53 500	1.6	0.3 ± 0.1

III. SIMULATED SAMPLES

Signal efficiencies and standard model backgrounds have been evaluated using fully simulated and reconstructed Monte Carlo events. The jet energies further received scale corrections and an additional smearing to take into account residual differences between data and Monte Carlo simulation, as determined with photon+jet events. The instrumental background from multijet production (QCD background) has not been simulated, and was estimated directly from the data.

A. Standard model background simulation

The processes listed in Table I are expected to be the largest contributors to standard model backgrounds in the acoplanar jet topology. They were generated with `ALPGEN` [4], interfaced with `PYTHIA` [5] for the simulation of initial and final state radiation, and of jet hadronization. The parton density functions (PDF's) used were `CTEQ5L` [6]. A Poisson average of 0.8 minimum bias events was superimposed. In order to avoid double counting among the various `ALPGEN` samples, the number of hadronic jets reconstructed from the generated particles was required to be equal to the corresponding number of partons requested whenever a similar sample with higher requested jet multiplicity was available. The next-to-leading order (NLO) cross sections were calculated with `MCFM` [7], except for $t\bar{t}$ production where Ref. [8] has been used.

B. Signal simulation

The production of scalar leptoquarks *via* the processes

$$q\bar{q} \text{ or } gg \to LQ\overline{LQ}$$

was simulated with `PYTHIA` with the `CTEQ5L` PDF's. An average of 0.8 minimum bias events was overlaid. The chosen leptoquark masses range from 80 to 140 GeV, in steps of 5 GeV. For each mass, 10,000 events were generated.

The NLO leptoquark pair production cross sections were calculated using a code based on Ref. [9], with `CTEQ6.1M` PDF's [10]. For the mass range considered, they vary from 52.4 to 2.38 pb. These nominal values were obtained for a renormalization and factorization scale equal to the leptoquark mass.

TABLE II: Numbers of data events selected and signal efficiencies for $m_{LQ} = 140\,\text{GeV}$ at the various stages of the analysis. The last two cuts were optimized.

cut applied	events left	efficiency (%)
Initial cuts	306 937	59.4
C1: leading jet $p_T > 60\,\text{GeV}$	206 116	48.7
C2: leading jet $\lvert\eta_{\text{det}}\rvert < 1.5$	160 323	46.8
C3: second leading jet $p_T > 50\,\text{GeV}$	48 979	24.8
C4: second leading jet $\lvert\eta_{\text{det}}\rvert < 1.5$	42 028	22.7
C5: both leading jet $EMF < 0.95$	40 821	22.3
C6: both leading jet $CPF > 0.05$	34 746	22.2
C7: exactly two jets	5 213	15.3
C8: $\not\!\!E_T > 70\,\text{GeV}$	492	11.8
C9: no isolated track with $p_T > 5\,\text{GeV}$	314	10.1
C10: no isolated electron with $p_T > 10\,\text{GeV}$	300	10.1
C11: no isolated muon with $p_T > 10\,\text{GeV}$	287	10.0
C12: $\Delta\Phi_{\text{max}} - \Delta\Phi_{\text{min}} < 120^\circ$	180	9.4
C13: $\Delta\Phi_{\text{max}} + \Delta\Phi_{\text{min}} < 280^\circ$	124	8.4
C14: $\not\!\!E_T > 80\,\text{GeV}$	86	7.0

IV. EVENT SELECTION

The selection cuts which have been applied in this analysis are listed in Table II, together with the numbers of events surviving at each step and with the evolution of the efficiency for a leptoquark mass of 140 GeV.

The kinematic cuts **C1** to **C4** reject a large fraction of the standard model and QCD backgrounds. They take advantage of the central signal production by requiring that the two leading jet $|\eta_{\text{det}}|$ be smaller than 1.5, where η_{det} is the pseudorapidity measured from the detector center.

In cut **C6**, a comparison of jet energies with their counterparts carried by charged particles is performed. The ratio CPF of the total transverse energy of the charged particles emanating from the primary vertex and associated with a jet to the jet transverse energy recorded in the calorimeter is expected to be close to zero either if a wrong primary vertex was selected, in which case it is unlikely that the charged tracks truly associated to the jet will come from the selected primary vertex, or if the jet is a fake one, in which case there should be no real charged tracks associated with it. The efficiency of this jet confirmation procedure was determined using back-to-back dijet events.

Cut **C7** is applied to suppress further the QCD background, which is enriched in multijet events by the acoplanarity requirement. The inefficiency associated with the rejection of events with more than two jets was evaluated, based on studies of jet multiplicities in real and simulated $Z \to ee$ events.

The purpose of cut **C8** is to bring the QCD and standard model backgrounds to similar levels. The final $\not\!\!E_T$ cut value (cut **C14**) was optimized as explained further down.

Cuts **C5** and **C10** are used to reject events likely to contain an isolated energetic electron. (EMF is the fraction of jet energy contained in the electromagnetic section of the calorimeter.) Together with cuts **C9** and **C11**, they reject a large fraction of events originating from the W/Z+jet processes.

The angular correlations between the jet and $\not\!\!E_T$ directions are used to suppress both the QCD and standard model backgrounds. To this end, the minimum $\Delta\Phi_{\text{min}}(\not\!\!E_T, \text{anyjet})$ and maximum $\Delta\Phi_{\text{max}}(\not\!\!E_T, \text{anyjet})$ of the azimuthal angle differences between the missing E_T direction and the direction of any of the two jets are combined as shown in Fig. 1. It can be seen in the top frame that cut **C12** rejects most of the remaining QCD background. Cut **C13**, which suppresses standard model backgrounds at the expense of a moderate reduction of the signal efficiency, was optimized as explained below. Its effect can be seen in the bottom frame of Fig. 1.

Finally, optimal values for the $\not\!\!E_T$ and $\Delta\Phi_{\text{max}} + \Delta\Phi_{\text{min}}$ cuts were determined as the ones which minimize the cross section expected to be excluded, on average, in the absence of signal. A leptoquark mass of 140 GeV was used for the signal efficiency. The $\not\!\!E_T$ cut values probed ranged from 60 to 90 GeV, in 10 GeV steps, and the cut on $\Delta\Phi_{\text{max}} + \Delta\Phi_{\text{min}}$ was varied between 260° and 300° in steps of 10°. For each set of cuts, the QCD background was estimated as explained below. The systematic uncertainties discussed further down were taken into account in the calculation of the expected limits. The optimal set of cuts reported as **C13** and **C14** in Table II selects 86 data events.

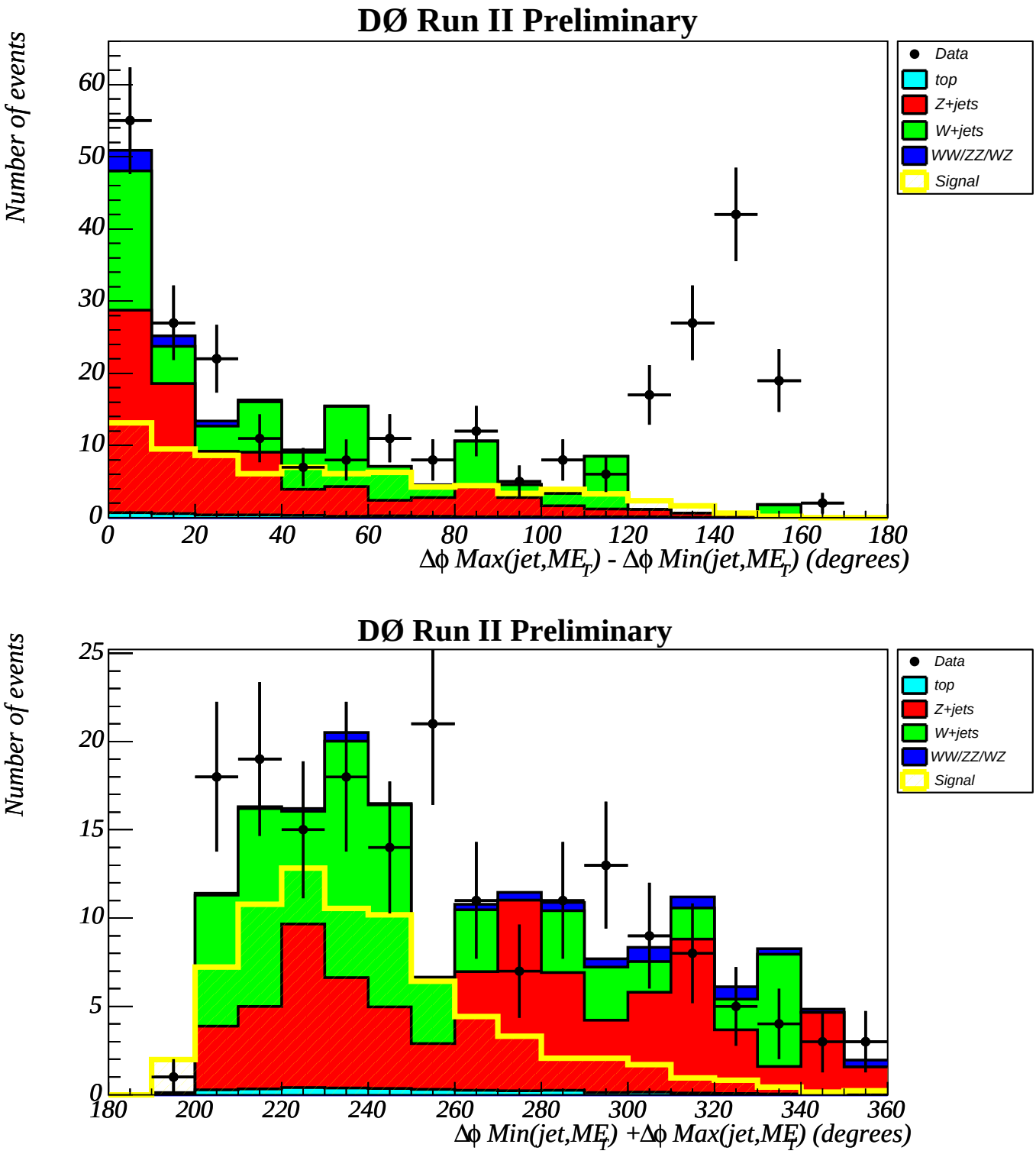

FIG. 1: Distributions of $\Delta\Phi_{\rm max} - \Delta\Phi_{\rm min}$ (top) and of $\Delta\Phi_{\rm max} + \Delta\Phi_{\rm min}$ (bottom) for data (points with error bars), for SM backgrounds (filled histograms), and for a 140 GeV mass LQ signal (empty histogram). In the $\Delta\Phi_{\rm max} + \Delta\Phi_{\rm min}$ distribution, the cut $\Delta\Phi_{\rm max} - \Delta\Phi_{\rm min} < 120^\circ$ has been applied.

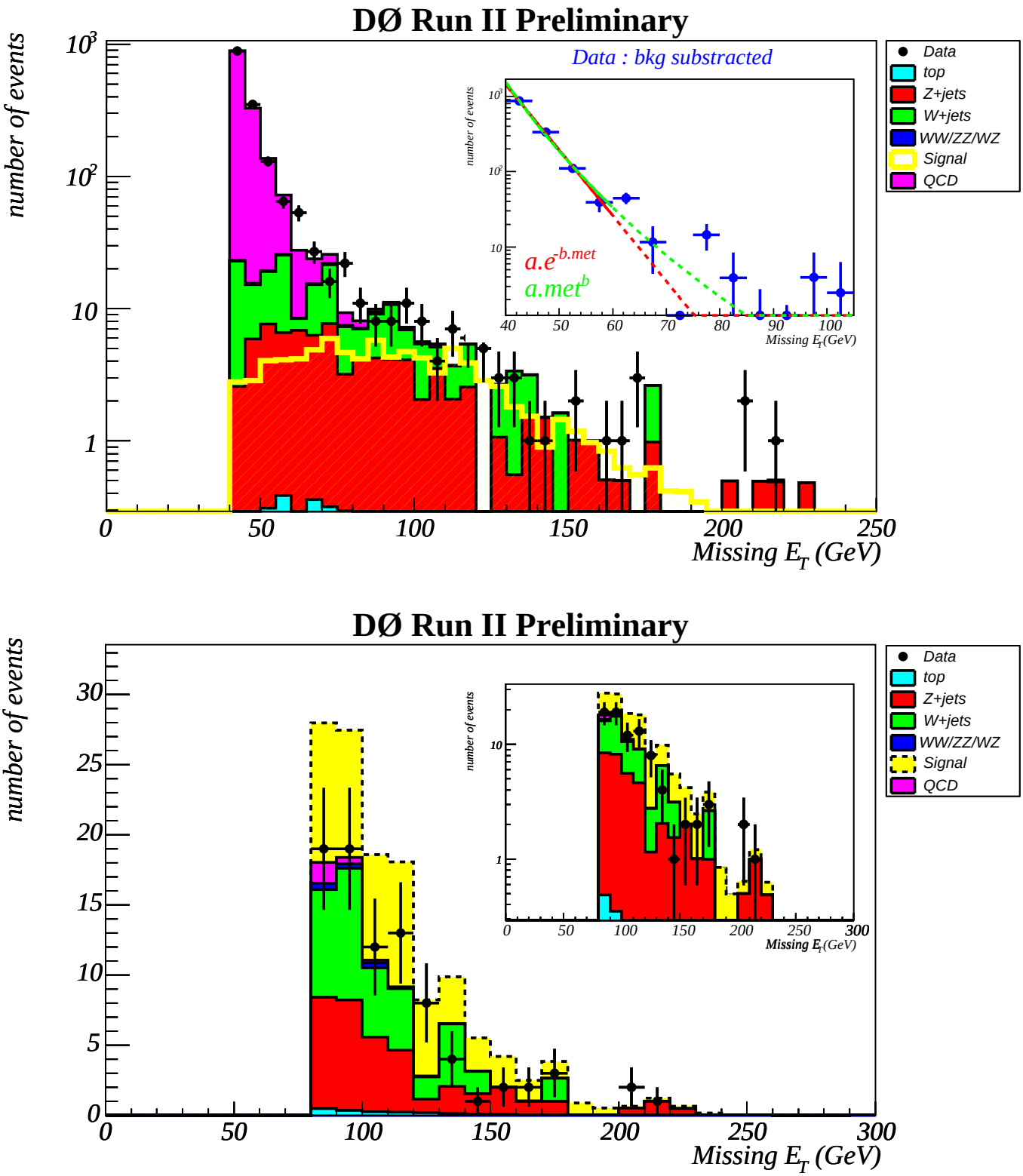

FIG. 2: Distributions of the missing transverse energy for data (points with error bars), for SM backgrounds (filled histograms other than purple and yellow), for the QCD background (purple histogram), and for a 140 GeV mass LQ signal. In the top frame, the LQ signal is shown as an empty yellow histogram, and the insert shows how the QCD contribution is estimated from power-law and exponential fits. The $\not\!\!E_T$ distribution in the bottom frame is final, with the same color code, but with the signal displayed on top of all backgrounds.

TABLE III: Standard model, QCD and total backgrounds expected; number of data events selected; and number of signal events expected for $m_{LQ} = 140\,\text{GeV}$, assuming the nominal production cross section. For the SM and total backgrounds, as well as for the signal, the first errors are statistical, and the second systematic. The error on the QCD background is mostly systematic from the difference between the power-law and exponential fits.

SM background	$72.9\ ^{+10.1}_{-9.7}\ ^{+10.6}_{-12.1}$
QCD background	2.3 ± 1.2
Total background	$75.2\ ^{+10.1}_{-9.7}\ ^{+10.7}_{-12.2}$
Events selected	86
Signal ($m_{LQ} = 140\,\text{GeV}$)	$51.8 \pm 1.8^{+5.6}_{-4.6}$

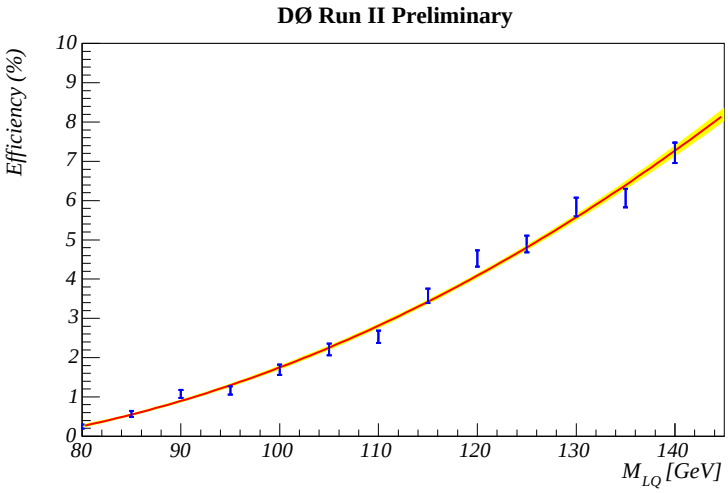

FIG. 3: Selection efficiency, in percent, as a function of the leptoquark mass. The errors are statistical only. A parameterization by a second order polynomial is also shown, together with its statistical errors.

V. BACKGROUNDS

The various standard model background contributions after all cuts are listed in Table I. The main contributor is, as expected, $Z \to \nu\nu + \text{jet jet}$. The QCD background was estimated from exponential and power-law fits to the missing E_T distribution (Fig. 2) in the range $[40, 60]\,\text{GeV}$, after subtraction of the standard model contribution. Both fits were extrapolated beyond the $\not\!\!E_T$ cut value, and the average of the two results was taken as QCD background estimate, with a systematic error accounting for the difference between the two fit results. The values of the standard model and QCD backgrounds are given in Table III.

VI. RESULTS

A. Signal efficiency

The evolution of the efficiency at the various stages of the analysis is given in Table II for $m_{LQ} = 140\,\text{GeV}$. For the events fulfilling all the selection criteria, the trigger inefficiency is smaller than 2%. The variation of the signal efficiency as a function of the leptoquark mass is shown in Fig. 3, together with a parameterization which is used to derive the final results. The number of signal events expected for a leptoquark mass of 140 GeV is indicated in Table III.

B. Systematic uncertainties

The following sources of systematic uncertainty are fully correlated between SM-background and signal expectations:

- the integrated luminosity of the analysis sample: $\pm 6.5\%$;
- the relative jet energy scale between data and simulation: $^{+4}_{-8}\%$ for the SM background, and $^{+6}_{-4}\%$ for the signal;
- the relative jet energy resolution between data and simulation: $^{+2}_{-4}\%$ for the SM background, and negligible for the signal;
- the trigger efficiency: $^{+0}_{-2}\%$ after all selection cuts.

In addition to the $^{+14}_{-13}\%$ statistical uncertainty of the simulation, the normalization of the SM-background expectation is affected by a 12% uncertainty, as inferred from a comparison of data and simulated $Z \to ee + 2$-jet events selected with the same criteria for the jets as in the analysis sample.

The uncertainty of ± 1.2 events on the QCD background was estimated from power-law and exponential fits to the $\not\!\!E_T$ distribution, as explained previously.

The signal efficiency depends on the PDF choice. Using the 40 eigenvector basis `CTEQ6.1M` PDF set [10], a $^{+6}_{-4}\%$ uncertainty was evaluated.

C. Limits

Given the number of selected events, the SM and QCD background expectations, the integrated luminosity of $310\,\mathrm{pb}^{-1}$, the signal selection efficiency as a function of the leptoquark mass, and the statistical and systematic uncertainties discussed above, a 95% CL cross-section upper limit has been obtained as shown in Fig. 4, using the CL_s approach [11]. The limit expected on average in the absence of signal is also indicated.

The nominal theoretical cross section for the pair production of scalar leptoquarks is also shown in Fig. 4. It was obtained based on Ref. [9] with `CTEQ6.1M` PDF's and for a renormalization and factorization scale μ_{rf} equal to the leptoquark mass. The uncertainty associated with the PDF choice was combined quadratically with the variation obtained when μ_{rf} is modified by a factor of 2 or 0.5. For a leptoquark mass of 140 GeV, the PDF uncertainty on the theoretical cross section amounts to $^{+18}_{-13}\%$ and the scale variation reflects in a change of $^{+11}_{-13}\%$, the quadratic sum being $^{+21}_{-19}\%$.

Taking into account the theoretical uncertainty, shown as a yellow band in Fig. 4, a mass lower limit of 136 GeV is derived at 95% CL. Masses smaller than ~ 85 GeV, to which this analysis is not sensitive, have been excluded previously.

VII. CONCLUSION

A search for acoplanar-jet final states in $p\bar{p}$ collisions at 1.96 TeV, performed in a data sample of $310\,\mathrm{pb}^{-1}$ collected by the DØ detector, revealed no deviation from the standard-model expectation. A mass lower limit of 136 GeV has been obtained for a single-generation scalar leptoquark decaying exclusively into a quark and a neutrino. While a tighter limit is available for third-generation leptoquarks [12], due to the increased signal purity achieved with heavy flavor tagging, this is the most stringent limit to date for first and second-generation scalar leptoquarks.

Acknowledgments

We thank the staffs at Fermilab and collaborating institutions, and acknowledge support from the DOE and NSF (USA); CEA and CNRS/IN2P3 (France); FASI, Rosatom and RFBR (Russia); CAPES, CNPq, FAPERJ, FAPESP and FUNDUNESP (Brazil); DAE and DST (India); Colciencias (Colombia); CONACyT (Mexico); KRF and KOSEF (Korea); CONICET and UBACyT (Argentina); FOM (The Netherlands); PPARC (United Kingdom); MSMT (Czech Republic); CRC Program, CFI, NSERC and WestGrid Project (Canada); BMBF and DFG (Germany); SFI (Ireland); Research Corporation, Alexander von Humboldt Foundation, and the Marie Curie Program.

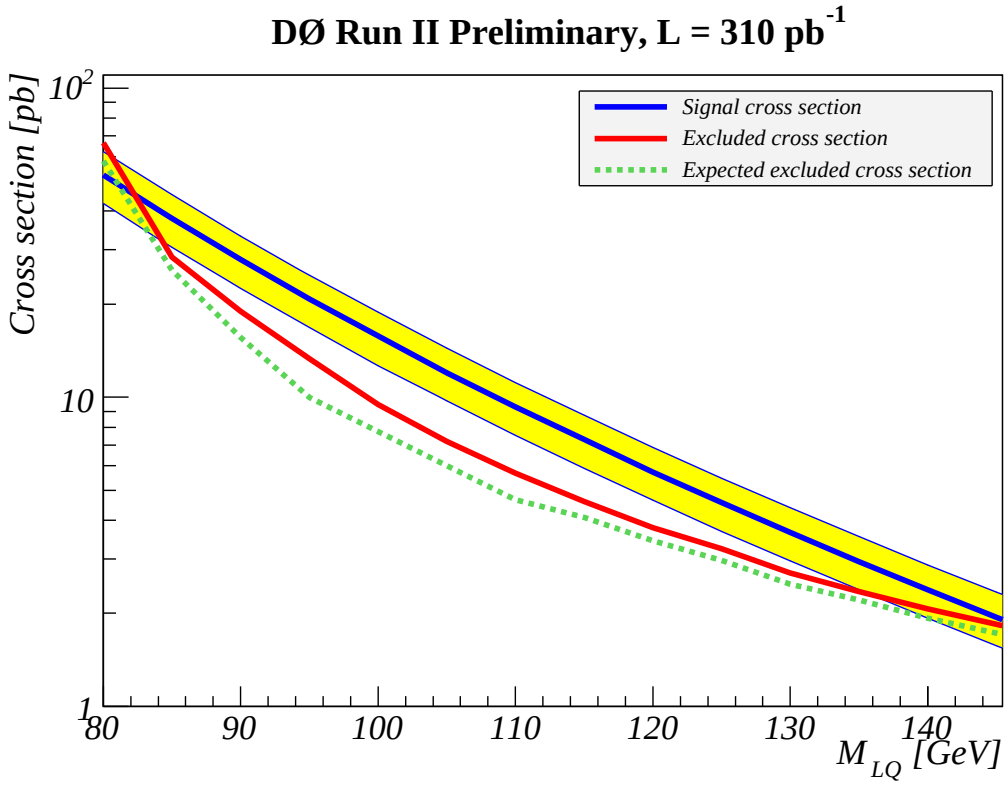

FIG. 4: Observed (red curve) and expected (dashed green curve) 95% CL cross-section upper limits as a function of the leptoquark mass. The blue curve represents the nominal cross section for scalar-leptoquark pair production. The yellow band indicates the uncertainty due to the scale and PDF choices. The leptoquark is assumed to decay exclusively into a quark and a neutrino.

[1] V. Abazov *et al.* (DØ Collaboration), *"The Upgraded DØ Detector"*, submitted to Nucl. Instrum. Methods Phys. Res. A.
[2] DØ Collaboration, *"Search for Scalar leptoquarks in the Acoplanar Jet Topology"*, DØ Note 4580-CONF, August 2004.
[3] D. Acosta *et al.*, Phys. Rev. D71, 112001 (2005), and Erratum ibid. D71, 119901 (2005).
[4] M.L. Mangano *et al.*, JHEP 0307, 001 (2003).
[5] T. Sjöstrand *et al.*, Comput. Phys. Commun 135, 238 (2001).
[6] H.L. Lai *et al.* Eur. Phys. J. C12, 375 (2000).
[7] J. Campbell and R.K. Ellis, Phys. Rev. D60, 113006 (1999).
[8] N. Kidonakis and R. Vogt, Int. J. Mod. Phys. A20, 3171 (2005).
[9] M. Krämer *et al.*, Phys. Rev. Lett. 79, 341 (1997).
[10] J. Pumplin *et al.*, JHEP 0207, 012 (2002); D. Stump *et al.*, JHEP 0310, 046 (2003).
[11] The ALEPH, DELPHI, L3 and OPAL Collaborations and the LEP Working Group for Higgs boson searches, R. Barate *et al.*, Phys. Lett. B565, 61 (2003);
T. Junk, Nucl. Instrum. Methods A 434, 435 (1999).
[12] T. Affolder *et al.*, Phys. Rev. Lett. 85, 2056 (2000).